Background

Face Detection

The seminal work on face detection is the Viola & Jones (2001) paper, which for the first time gave reliable detection while maintaining a speed capable of real- time use. These advances were due to a combination of different techniques. Firstly, the use of the "integral image" in order to greatly reduce the number of lookups to find the sum intensity of a region in an image, requiring only four reads for an area of any size. An integral image is essentially a cumulative map of the pixel intensities, such that the value at any position tells the sum of those pixels to the top left of it (Figure 1). By reading the four corners of a rectangle in an integral image, we can cancel out the area to the top and left, leaving only the sum of the area inside the rectangle (Figure 2). This makes it easy to compare the relative intensities of areas in images, which is fundamental to the features chosen by Viola and Jones, the Haar features (so named due to similarity with Haar Wavelets). Haar features compare the difference in brightness between regions of rectangles, in an attempt to pick up contrast variation. The feature value is the white region minus the shaded region of the rectangles in the figure. A 24×24 window is typically used for face detection, and during detection the values of Haar features at specific positions and sizes within that window (determined in the learning stage) need to be computed.

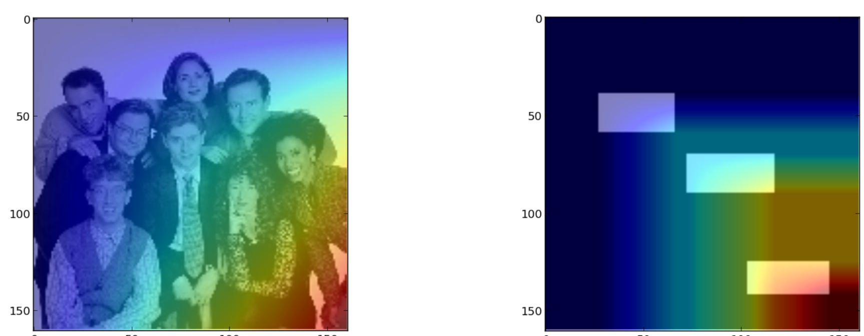

Figure 1: Visualisation of the integral image for two different pictures, as a colour map of the integral value superimposed on the original image. The value of the integral image at any location is the sum of all the pixels to the top left of it. This is apparent in the right image, where we have several white rectangles (pixel value 255) on a black background (pixel value 0), causing sharper changes.

Accounting for all variations in position and size (x,y,w,h) within the window there are many thousands of possible features. In order to pick a small number that

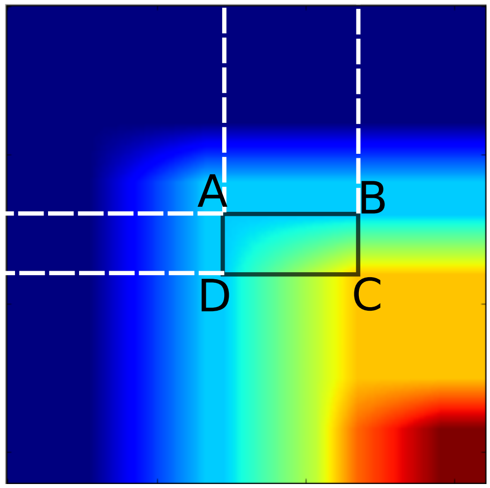

Figure 2: Finding the sum of intensities of a region with the integral image, using the second picture of the previous figure. Each point gives the sum of the pixel values to the top left. If we take point C then we want to “cancel out” the excess area outside the rectangle. We can subtract B and D, but then we have taken too much, since the area top-left of B and D overlap. Therefore we have to add A to get the right value. The sum of the area in the rectangle is then C-D-B+A.

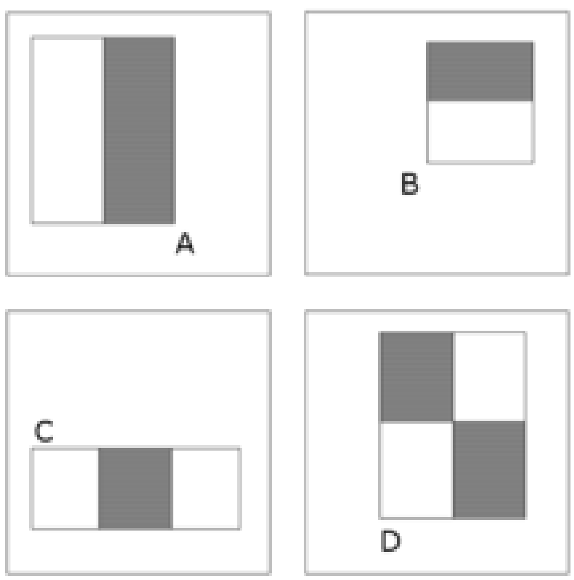

Figure 3: Types of Haar Features (within larger windows) (Wikipedia/Public Domain)

are good for classifying, the method of Boosting is used (specifically AdaBoost), which allows multiple weak classifiers to be combined into one strong classifier. A weight is associated with each training sample, initially all equal, and the feature which best discriminates between the positive and negative samples is chosen. The weights are then updated such that missclassified samples using this feature are given a higher weight, and correct samples a lower one (so more effort goes towards "fixing" the missclassifications), then the feature selection is repeated with the new weights. In the end we get an ensemble of features that combined have a lower error.

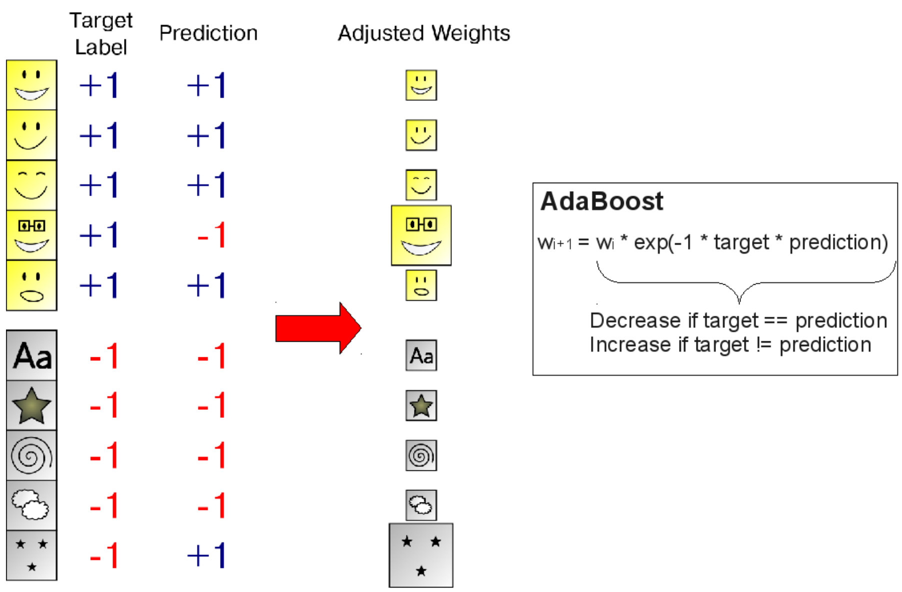

Figure 4: A visual illustration of Adaptive Boosting (AdaBoost), and the weight update step ((Thewlis, 2012))

However, with the above, during detection all the chosen features will need to be computed for all the window positions. Viola and Jones noticed that this could be improved by having a cascade of different boosted classifiers, which are decent at rejecting non-faces but will rarely reject a true face, chaining these classifiers together such that a rejected window will be immediately discarded, but an accepted window will be passed on to the next level in the cascade to face further scrutiny. This means that normally only the windows with true faces need go through every single level, whereas a non-face may be rejected right from the start. This avoids examining every single chosen feature for every single window, and makes sense intuitively since the vast majority of windows in most images will not have a face, so it is beneficial to reject them early, speeding up the procedure.

A widely used implementation of Viola Jones face detection is the OpenCV

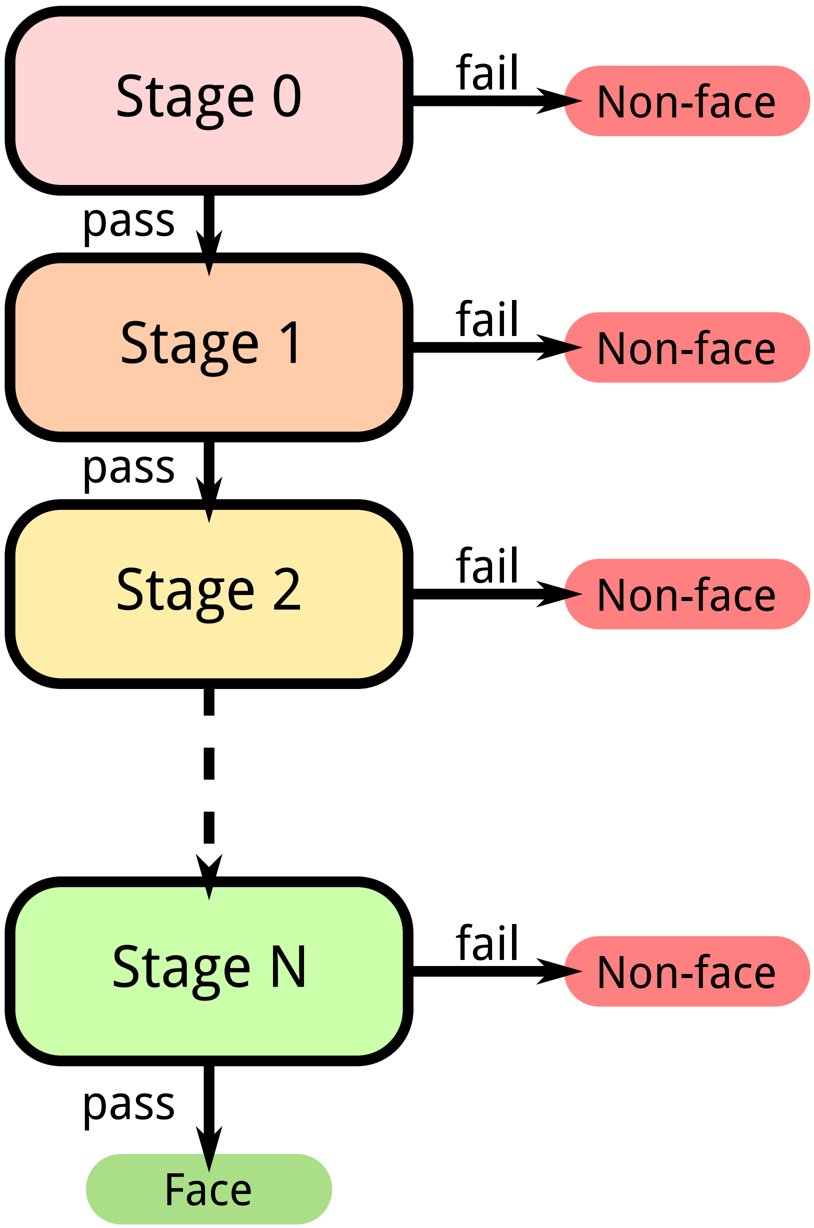

Figure 5: The Cascade Structure. Suspected non-faces are rejected immediately, potential faces go on to further stages

library, which provides several pre-trained cascades in an XML serialisation format. Many of the javascript face detection solutions are based on OpenCV's code.

Lienhart Lienhart & Maydt (2002) proposes an extra set of "tilted" Haar features at 45 degrees, computed thanks to a rotated integral image, in order to better represent distinctive characteristics such as slanted edges which would otherwise be missed.

Besides Haar features, another mechanism that can be used is Local Binary Patterns (LBP). Originally used for pattern description by Ojala, Pietikhenl & Harwoodet al. (1994), the basic LBP simply describes the neighbourhood of a pixel in terms of whether the 8 surrounding pixels are darker or lighter than the central one, and going clockwise from the top, can be represented as an 8 bit number by writing 1 if the center is lighter, 0 otherwise.

Zhang, Chu & Xianget al. (2007) extended LBP to a multi-block representation, dividing a rectangle into 3x3 blocks and comparing the outer ones with the centre, for use with face detection. Properties of LBP are that it is more robust to illumination variation, since it only records the lighter/darker relationship rather than a quantitative amount like with Haar. The ability to represent the configuration of an LBP rectangle in just one byte also makes it space efficient, especially useful when GPU textures are involved, since one could pack four patterns in one "pixel".

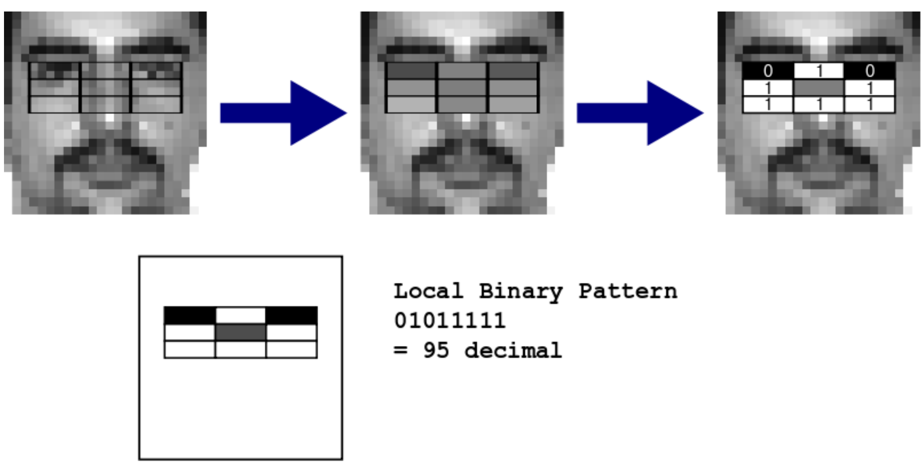

Figure 6: Local Binary Patterns for face detection

OpenCV also includes an LBP face detection implementation, along with a pre-trained XML file specifying a cascade for detecting frontal faces. It differs from the Haar cascades in that, for each weak classifier in a stage, rather than a simple threshold there is a list of the possible patterns (0 to 255) that contribute either positively or negatively towards a candidate window being a face, represented internally as a bit vector of size 256, made up of 8 32 bit integers.

[TODO explain LBP, advantage on GPU]

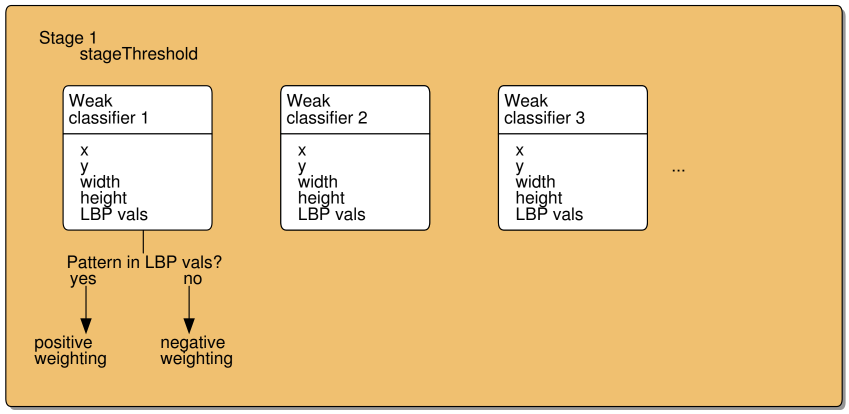

Vision in the Browser

The desire to integrate Computer Vision with the web has some history. Existing approaches largely make use of custom browser plugins able to run native code, such as the face detection used in Google Hangout @GoogleAPI. This has the disadvantage of requiring the user to trust and install the plugin in question, or may rely on browser-specific technology such as Microsoft's ActiveX or Google's Native Client. Adobe Flash has proved another contender Bonext (n.d.), being a commonly installed plugin able to provide access to the webcam, but its bytecode-based VM is slower than native code, and its popularity is waning due to incompatible mobile devices and the introduction of comparable features in the HTML5 specifications.

JavaScript, the de-facto language of the web, has been applied to certain vision tasks with some success. Despite the disadvantage of being an interpreted language, recent efforts towards speeding up JavaScript engines, such as Google Chrome's V8, have led to great improvements through techniques such as JIT ("Just In Time") compilation. Another leap forward in making JavaScript suitable for Vision was the "getUserMedia" API, introduced in 2011, giving JavaScript direct access to the user's webcam (upon consent). There are existing implementations of single-image face detection in JavaScript, such as Liuliu (n.d.), and there is the more amusing cat face detector Harthur (n.d.). Face detection on video is also possible, but typically employs techniques such as downsizing the video or skipping frames. Upon embarking on the present project, the author could locate no similar such endeavour to implement a Vision suite in JavaScript, but fate being as it is, a similar project by the name of "jsfeat" Inspirit (n.d.) appeared on the scene within a couple of weeks. The author chooses to take this as proof of current demand for vision on the web. Since jsfeat does not include GPU acceleration, it will serve as a useful baseline. In demonstrations on the web, when set to use the full range of scales, it can detect faces at around 27 fps, although it is working on input images of 160x120 resolution, and then using a "step" so that it skips every other pixel at the finest scale, and this step increases for larger scales.

The effort to give JavaScript standards-based access to computational and graphical libraries that can take advantage of dedicated hardware was pioneered by the Khronos group, maintainers of the OpenGL and OpenCL specifications. These libraries are commonly used in native programs for 3D graphics and parallel computation respectively.

In 2009 Khronos began to draft a specification for WebGL, which would give JavaScript 3D drawing capabilities, through an extended context of the "canvas" element which was introduced in version 5 of the HTML specification. WebGL is based on the OpenGL ES 2.0 specification, which itself is a cut down version of OpenGL initially designed for the benefit of mobile devices, lacking OpenGL's deprecated fixed rendering pipeline (which has built in support for lighting and perspective transforms) to give a more lightweight library, leaving it to the developer to explicitly specify vertex transformations and texture values needed to render a scene. WebGL's functions and behaviour are largely identical to OpenGL ES 2.0, so resources and documentation are often applicable to both. Some additional considerations are needed for the browser-based host such as security restrictions on image access and support for web-specific data types like HTMLVideoElement for grabbing texture from a video (eg. from a webcam) on the page. The specification for WebGL 1.0 was released in 2011 and experimental support is present in the latest versions of Google Chrome and Mozilla Firefox. Safari and Opera also support WebGL although it is currently disabled by default. Microsoft's Internet Explorer does not support it, unless third party plugins are used.

Following WebGL, work was started on a WebCL specification, providing JavaScript bindings to the OpenCL parallel computation library, to allow code to be sped up using hardware on the GPU or multi-core CPU, a use case being physics calculations in games. Although it is still in draft form, implementations have been released by Nokia and Samsung in the form of browser plugins. WebCL would certainly be a strong candidate for Vision related tasks in the browser, especially given the wide use of OpenCL and Nvidia's CUDA for implementing high performance Vision systems. However, it is not yet implemented natively in any browser, and it remains to be seen whether it will be adopted by browser manufacturers. Since the goal of this project is to implement Computer Vision in current browsers with no extra steps required on behalf of the user, at the moment WebCL is unfortunately not an option, and its cousin WebGL is the only viable choice for running code on the GPU from a browser.

Despite being intended for drawing 3D graphics, OpenGL and hence WebGL is quite capable for performing arbitrary calculations, due to the use of shaders, which are programs that run on the GPU for the purpose of modifying the geometry and colour of a scene. Using OpenGL for arbitrary computation seems to have become quite fashionable around 2005, as evidenced by the number of pages dedicated to it in the GPU Gems 2 book, but then seems to have fallen out of favour after NVIDIA released CUDA in 2007, giving a more convenient purpose-built framework for computation in the GPU. Nevertheless, with the rise of OpenGL ES in smartphones and WebGL in the browser, using GL for computation remains attractive. In OpenGL there are two types of shader, vertex shaders, which specify the geometrical position in 3D given an array of vertex points and vertex-specific attributes, and fragment shaders, which specify the colour (RGB and alpha transparency) of the output pixels after rasterisation. Shaders in OpenGL are written in GLSL (The OpenGL Shader Language) a C-like language which offers many of the conveniences found in computation-oriented GPU platforms such as CUDA. An advantage of handling computation in shaders is that they operate in a parallel, computationally independent manner on many vertices or pixels, essentially the SIMD (Single Instruction Multiple Data) paradigm. This offers a large advantage over sequential computation on the CPU, provided the algorithm can be structured in such a way as to take advantage of massive parallelisation over many data elements, as is often the case with image processing algorithms where a certain operation is desired to be performed on every pixel. The fragment shader is where the main potential for parallelisation over data lies, since it can look up data in textures, run procedures, and output a value for every pixel in the canvas. However, computation in the vertex shader can also be valuable, since it precedes the fragment shader in the OpenGL pipeline and is able to pass data to it in the form of "varyings", which are vertex-specific variables then interpolated across the rasterised surface. This gives the possibility to precalculate information in the vertex shader that will be used by many pixels.

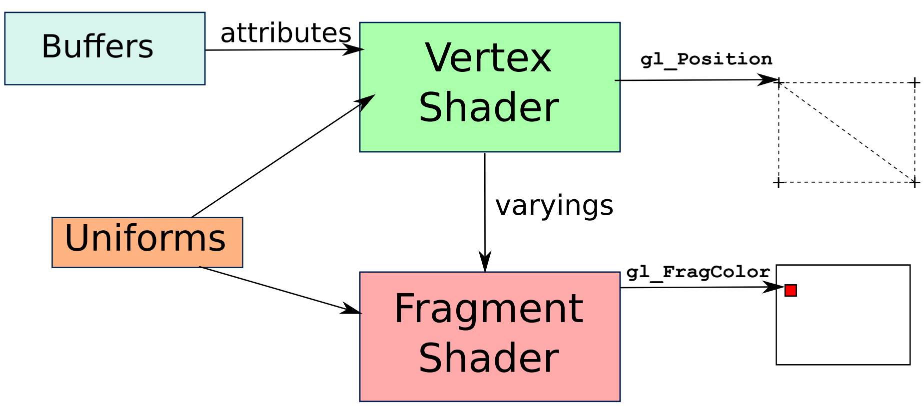

Figure 7: The WebGL pipeline

So far we have been talking about pixels and 3D vertices, which are not very useful if we want to work with 2D images or arbitrary numerical data. The trick to getting a simple 2D surface is to render a viewport-aligned rectangle (in practice, by drawing two triangles). As Tavares (2011b) describes, WebGL is essentially a 2D API if we want it to be, and we can work in pixels rather than OpenGL's "clipspace" units (which are -1.0 to 1.0) by normalising by the canvas resolution. As for passing data to the shaders, a limited amount of floating point or integer variables and arrays may be passed as "uniforms" to the shaders (which remain constant for each vertex or pixel), but for handling large data such as images and arrays textures must be used. Instead of drawing to the screen, the output may be rendered to a framebuffer with a texture attached, allowing it to be used as an input texture for another stage. Each pixel in a normal texture is 4 bytes (RGBA), which is suitable for representing some numerical data, but in many cases it is preferable to use floating points. This can be done using the WebGL extension `OES_texture_float`, which is supported on most platforms. However, until recently, there was no defined way to read back floating point values to JavaScript, requiring inventive solutions such as packing floats into bytes Lab.dev.concord.org (n.d.). The latest draft specifications of `EXT_color_buffer_half_float` Khronos (n.d.) and `WEBGL_color_buffer_float` Khronos (n.d.), amend the readPixels() function to permit float types, however it will be a matter of time before all browsers support it. In addition, when doing calculations, care should be given to the precision qualifiers offered by GLSL (highp, mediump, lowp) which alter the precision of numerical representations, at a speed/accuracy tradeoff. Per the GLSL specification, highp (normally IEEE float) may not be available in the fragment shader, and integers may be implemented as floats in the hardware, which should be taken into account when implementing algorithms.

There are various examples on the web using WebGL to improve the efficiency of calculations in simulations, such as WebGL Water Wallace (n.d.) which calculates the water and caustics simulation in the shaders,

In addition, the trick of using of OpenGL Shaders to increase performance is employed by the GPUImage library Larson (n.d.) for image processing on iOS devices.

Computation in WebGL - concepts and example

We shall provide a gentle introduction to the concepts behind using WebGL to perform general purpose computation, walking the reader through the main steps required to implement a simple convolution shader which operates on images from the webcam. Although this is a somewhat simple image processing task, it introduces many of the techniques that will be essential for face detection. Indeed, the act of processing a stage of the face detection cascade within a window can be viewed as a sort of glorified convolution, since for a certain pixel location it consists of looking up the values within some surrounding neighbourhood, using them to determine what result to output.

We lean on the work of Tavares (2011c) in using WebGL for image processing, and draw on Harris (2005) in order to explain computational concepts in terms of OpenGL, in particular we make use of the analogies presented between CPU techniques and their GPU counterparts. We shall also make use of a JavaScript library, called WebCV, created by the author for the purpose of abstracting away some of the complications of WebGL, providing utility functions which facilitate tasks commonly needed for general purpose computation and computer vision applications.

Before we can start using WebGL, we must first make some preparations. WebGL is exposed through a special context of the HTML `<canvas>` element, so we insert a canvas in our document, specifying the width and height. To access the webcam, we also require a `<video>` element, which we set to the same dimensions as the canvas. The body of our HTML document then looks as follows.

```
<body>
<canvas id="glcanvas" width="400" height="300"></canvas>
<video id="webcamvideo" autoplay width="400" height="300"></video>
</body>
```

We must now use JavaScript to give some life to these elements. We want to initialise the WebGL context of our canvas, and make it so our video receives input from the webcam. For the former we can instantiate our WebCV library using `WebCV.create(canvas)`, passing in our canvas, which returns an object (which we shall call `cv`) through which we can access our utility functions. The bare WebGL API is also available through `cv.gl`. This level of indirection allows us to instantiate multiple copies of WebCV on different canvas elements, each with their own WebGL context. To receive video from the webcam we use the browser's `getUserMedia` API, for which we have a wrapper available in `cv.utils.getUserMedia` to abstract away from the browser- specific differences. This will cause a prompt to appear to the user, asking for permission to use their webcam, and call a specified function upon success. Within this function we then set the `src` of the `<video>` element, which causes it to start streaming video from the webcam.

```
// Get our canvas object
var canvas = document.getElementById("glcanvas");

// Initialise WebCV, which in turn initialises WebGL
// We make cv and gl global variables
cv = WebCV.create(canvas);
gl = cv.gl;

// Ask for the webcam
cv.utils.getUserMedia({video: true},
                      function(stream) {
                          var vid = document.getElementById("webcamvideo");
                          vid.src = stream;
```

```
                },
                function () { alert("Couldn't get webcam"); });
```

We now look at the roles of shader programs in WebGL. We have two types of shaders, the vertex shader and the fragment shader. If we were using WebGL to draw 3D geometry, the vertex shader would answer the question "Where should my vertices be placed?", by setting the value of `gl_Position`, and the fragment shader would answer the question "What colour should my fragments (pixels) be?", by setting `gl_FragColor`.

Recall we have three special types of variables in our shader programs. Uniform variables can be treated like global variables. They can be set from JavaScript, and are accessible from both the vertex and the fragment shader. They are the most straightforward way of setting variables which we use in the shader, and are used for values that do not vary according to the position in the image. For example, to convolve the image with a 3×3 matrix as the kernel, we would use a Uniform variable to hold the matrix, since we need the same matrix for every pixel, but can change the matrix for different uses of the shader program.

Attribute variables are used in the vertex shader for accessing vertex- specific data. They are specified by uploading arrays to buffers on the GPU. A primary use of attribute variables is to set the *vertex coordinates* used to determine the position of vertices, and the *texture coordinates* which define a mapping of vertices to positions within texture. Following Tavares (2011b), to draw a rectangle in 2D we need to draw two view- aligned triangles, as in Figure 8 (since the triangle is the only polygon primitive available in OpenGL ES and WebGL). This gives six coordinates for the vertices, each with two elements (x, y), so we would have to upload a buffer of 12 elements.

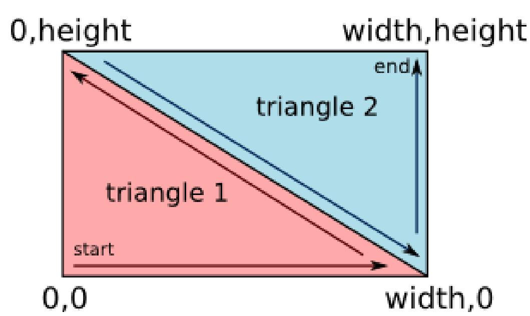

Figure 8: Drawing a quad using two triangles, showing the order of the vertices are specified.

The analogy given by Harris (2005, p.502) for the *vertex coordinates* is that they specify the *computational range*, by determining which pixels will be generated. We typically only wish to draw a rectangle (2 triangles), for which the task of the vertex shader is fairly simple, we just want to pass through the vertex

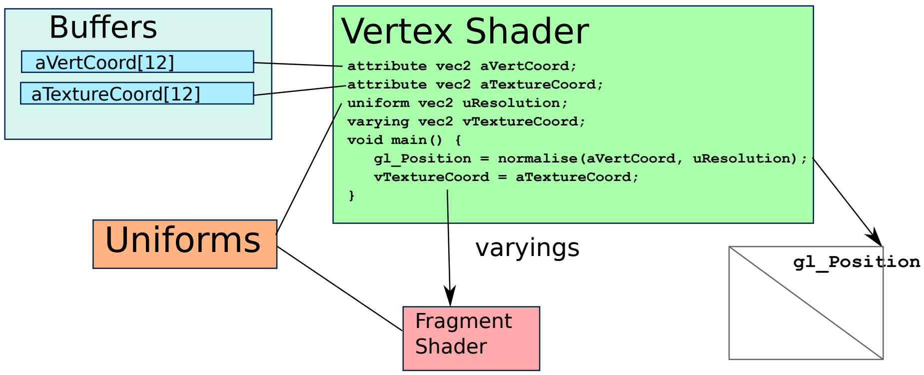

Figure 9: A simple vertex shader to draw in 2D

coordinates, as if we were drawing pixel positions directly. A schematic of this simple vertex shader is shown in Figure 9, and it can be used whenever we just want to draw things in 2D and forget we are dealing with a 3D graphics API. Its only job is to draw the 2D geometry specified by our vertex coordinates, as if by orthogonal projection, and pass our texture coordinates to the fragment shader. The details of the normalisation of the input vertex coordinates in pixels to output vertex positions have been omitted, and require some understanding with OpenGL's coordinate systems, explained in [TODO appendix coordinates].

While the *vertex coordinates* represent the *computational range*, the *texture coordinates* can be considered our *computational domain*. Texture coordinates in WebGL are 2-element floating point vectors varying from 0.0 to 1.0 in each dimension, and similarly to the vertex coordinates are passed as an attribute to the vertex shader using a buffer. However it is the fragment shader which needs to access the texture, not the vertex shader. This is where the third special type of variable, the varying, comes in to play. Varying variables output from the vertex shader at each vertex are linearly interpolated across the fragments between the vertices (this can be seen graphically in Figure 11). So while we only specify the texture coordinates at each vertex, by using varyings the texture coordinates passed to the fragment shader can span the entire texture. In many cases we will want the computational domain and range to be equal, in which case we can use a texture the same size as our output drawbuffer. However texture coordinates give us the flexibility to have a domain and range of different sizes, for example we may do some data minification that consumes two pixels in order to output a result. In the case that the domain and range are equal (or the domain can be expressed as offsets of the fragment position), we can avoid using texture coordinates through the use of the special `gl_FragCoord` variable in the fragment shader, which contains the screen- space position of the current fragment (already offset by 0.5 to give the centre of the fragment). We can then divide this by the texture size to get a 0.0-1.0 texture coordinate. An alternative way to modify the computational range is to use the `gl.viewport` and `gl.scissor` comands. The first modifies the size of the viewport, and the second lets us specify a box such that only the pixels within the box are written.

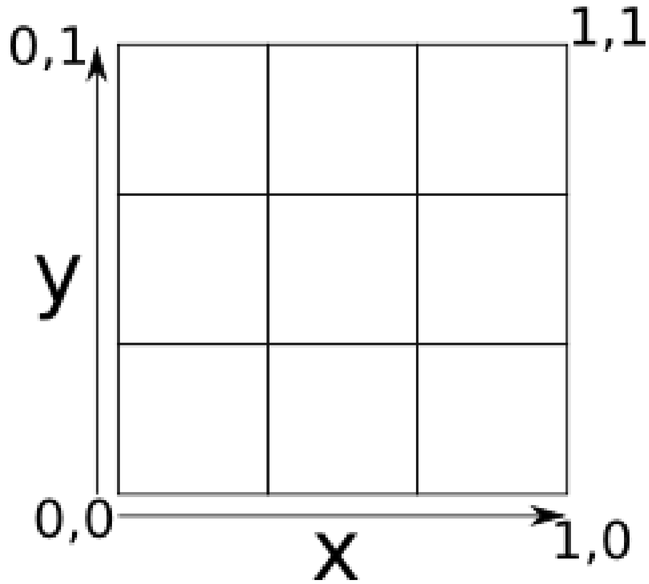

Figure 10: A texture of 3x3 texels. Texture coordinates in OpenGL vary from 0,0 to 1,1 regardless of size.

We now come to the main powerhouse in our inventory of WebGL tools, the fragment shader itself. The fragment shader is useful because it runs for every pixel (or fragment), thus making it amenable to parallel computation on a grid, where the output at one pixel does not require any intermediate information computed by its neighbours. The analogy with the CPU given by Harris (2005) is that fragment shader programs can be treated like the inner loops when iterating over our elements. So while on the CPU to process the elements of a grid we would have to loop over the X and Y indices, and have some core processing in the middle, it is this core that would be well suited to the fragment shader when converting code to run on the GPU. Woolley (2005) extends this analogy to explain that many of the performance considerations we would typically have in mind when writing the inner loop of an algorithm on the CPU are equally valid when considering the code in our fragment shader. Primarily, we want to put as little code as possible in the fragment shader itself, and pre-compute variables outside the fragment shader where possible, to avoid re- calculating redundant values for every fragment. The expense of inner-loop branching is likewise a pitfall on the GPU, even more so because it prevents efficient instruction-level parallelisation by the GPU hardware. However, this said, often the shader compiler in modern graphics drivers is clever enough to optimise away apparent inefficiencies, and especially compared to JavaScript, putting redundant computation in the fragment shader may be faster, so the only real

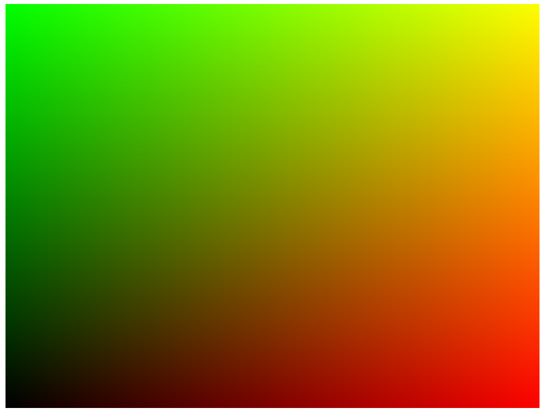

Figure 11: Interpolation of texture coordinates, shown by outputting the x and y texture coordinate in the red and green colour channel, such that we get a gradient that varies linearly in each channel

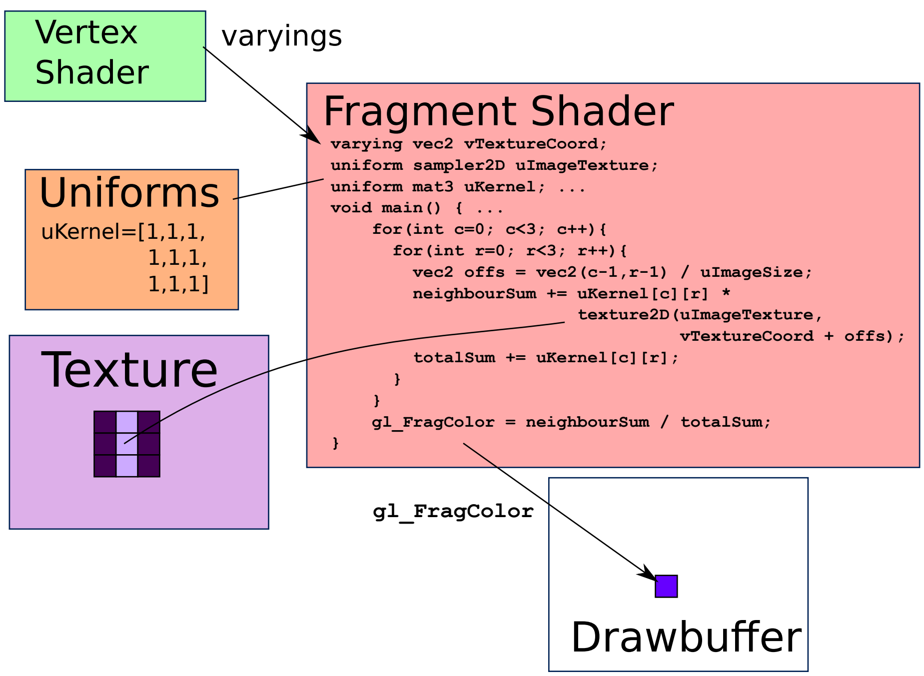

Figure 12: Fragment shader to process our convolution kernel. The example convolution kernel given would simply compute the average of the nine texels in the neighbourhood, giving a blur effect.

way to know is to profile and test.

For our convolution example, the fragment shader is where we do the main work, shown in Figure 12. We have our kernel to convolve with passed in as a uniform 3×3 matrix (bearing in mind the OpenGL matrices are column-major), and our texture coordinates passed from the vertex shader give our centre texel. Convolving is then a matter of accessing the 9 texels in the neighbourhood and computing a weighted average using the values from the kernel, which is easiest to do with a couple of `for` loops. (We might think it faster to unwrap these loops and specify the texture coordinates offsets individually, but the compiler likely does this already.) We output our weighted average by assigning it to `gl_FragColor`, which causes this pixel colour to be output during rasterisation. We can observe the effect of several convolution kernels in Figure 13, along with an application for edge detection.

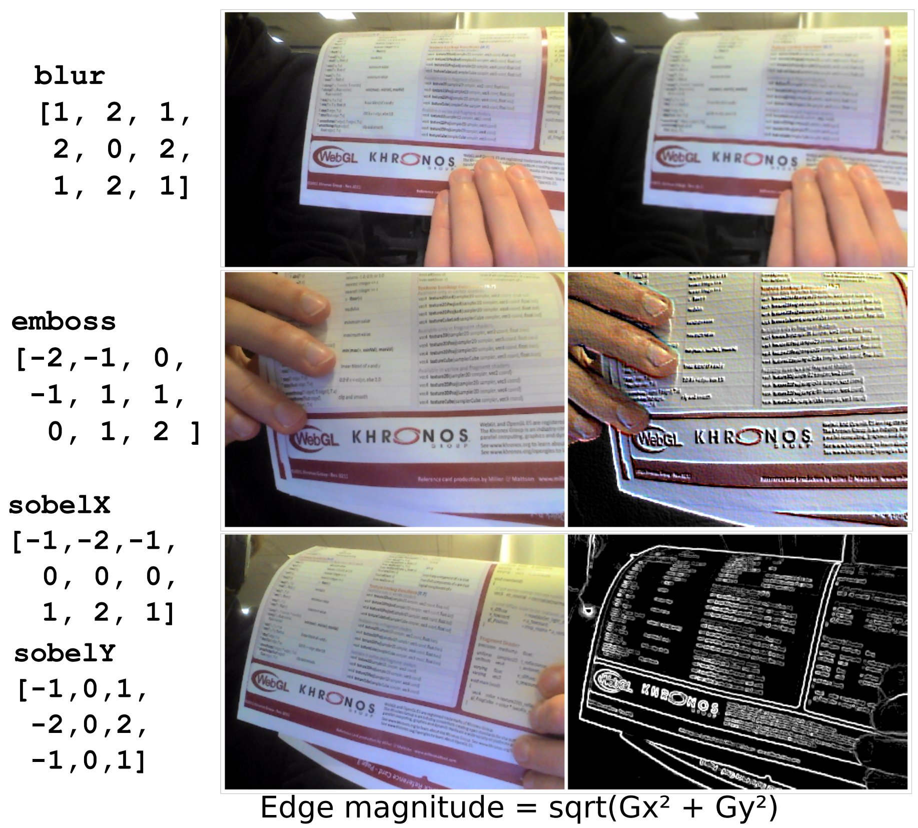

Figure 13: The effects of convolution using different kernels. We also show an application of convolution for edge detection, where we use the two sobel kernels to find the edge gradient in the X and Y direction, Gx and Gy respectively, and then output the magnitude of this gradient, showing edges in the image.

Convolution can be seen as a *gather* operation, since we are obtaining data from nearby locations in our grid of pixels, looking up values in texture memory. We prefer that our computations be structured as a gather, since fragment shaders are well suited to gathering, but it is impossible to perform *scattering*, which is when we write out to different locations in memory, distributing values to other elements in the grid. The fragment processed can only write to precisely one location. As described in Buck (2005), if we require a scattering operation, the first step should be to see if it can be converted into a gather. Techniques for dealing with scattering include adding a layer of indirection, by outputting an address along with our output value, which can then be processed by later passes to give a contiguous array.

Once we have the shaders set up, launching our computation is then just a matter of drawing geometry with the `gl.drawArrays(gl.TRIANGLES, 0, 6)` function, which will draw the six vertices of our triangles. To run in real time using images from the webcam, we use the browser's `requestAnimationFrame` to call our drawing code at appropriate intervals. This relatively new function avoids the problems of JavaScript's `setInterval` function, which can be used for executing a function periodically, but has no knowledge of framerate, and will keep on running even when the window is not visible, wasting resources. Nevertheless, for browsers that do not support `requestAnimationFrame`, we offer a wrapper function that falls back to `setInterval`. In order to make all our shaders available through JavaScript, we have a Python script that constructs a JavaScript object containing all the shader source code, and a function `cv.getNamedShader` which deals with the task of compiling and linking our shader programs. We also provide functions in our WebCV library to deal with setting uniforms, uploading buffers, creating textures etc., allowing us to specify an associative array containing the uniform or attribute names with values as native JavaScript arrays or numbers, automatically dealing with the messy task of calling the correct version of many related functions, such as `uniform1f(), uniform2f(), ... uniform4iv() etc` which set uniforms of different types and sizes.

By now we are able to show the results of the convolution in our canvas on the screen, but we would also like to be able to use the results of previous computations in subsequent stages. For example, we might like to chain together multiple convolution passes. For this we use a framebuffer, which allows us to render our output to a texture. A framebuffer itself is just a lightweight structure, containing multiple attachment points, to which we attach objects containing storage, that we can render into. The attachment point used for storing the pixel colours drawn is `COLOR_ATTACHMENT0`, to which we can attach a texture whose values can then be accessed in subsequent fragment shaders. Another type of attachment is the `DEPTH_ATTACHMENT`, to which we can attach a depthbuffer, which will turn out useful later. Because we cannot read from the same texture that we are rendering to, if we want to use a pipeline of shaders it is necessary to use the "ping-pong" technique, alternating between two different framebuffers, such that one is used as the render target and one has its texture read by the shader, then swapping roles so that the output from the previous pass can be fed into the next one. Lastly, if we want to read back data into JavaScript, we can use the `gl.readPixels` command, which copies the contents of the current framebuffer's texture into a JavaScript array. Because this can be slow, it is best to do all computation possible on the GPU before reading back at the end.

Implementation

Cascade

Javascript Implementation

The core of the face detection method used is the cascade structure described in [TODO], which subjects each window to progressively harder tests, each test being a stage in the cascade which specifies a number of weak classifiers with corresponding Local Binary Pattern features within the window.

Although the precise nature of these weak classifiers is crucial when constructing a cascade from training images (using the statistical method of Boosting to construct a strong classifier from individual classifiers performing only slightly better than chance) for the purposes of detection we need not be overly concerned with this. From a more abstract point of view, the weak classifiers simply tell us which points we need to look up in the integral image and which values should be used in the subsequent arithmetic in order to determine whether a window passes a stage. The main challenge then is to do this as fast as possible.

We initially implement the cascade using only JavaScript, running on the CPU, to give us a reference implementation which can then be used to assess the correctness of a WebGL version running on the GPU. For the moment we only consider the base scale of the cascade, 24×24 pixels, meaning we can only detect faces which occupy a window of these dimensions. We use the XML cascade file `lbpcascade_frontalface.xml` from the @OpenCV project, however we first use a Python script to convert this to a format more suitable for use with JavaScript, JSON (JavaScript Object Notation) which allows us to treat the cascade as a native JavaScript data structure, made up of JavaScript objects (associative maps with string keys, of the form `{"key": value}`) and arrays (eg. `[v1,v2,v3]` where values can be any type, not necessarily homogenous). An example of this data structure is given below, showing just one stage with one of its weak classifiers

```
var lbpcascade_frontalface = {
    "width": 24,
    "height": 24,
    "stages": [
        // 1st Stage
        {
            "stageThreshold": -0.7520892024040222,
            "weakClassifiers": [
                // 1st Weak classifier
                {
                    "featureRectangle": [6, 5, 4, 3],
                    "leafValues": [-0.654321014881134, 0.8888888955116272],
                    "categoryBitVector": [
                        -67130709,
                        -21569,
                        -1426120013,
                        -1275125205,
                        -21585,
                        -16385,
                        587145899,
                        -24005
                    ]
                }
                // ...2 more weak classifiers in this stage
            ]
        },
    // ...19 more stages (having up to 10 weak classifiers each)
    ]
}
```

Essentially, we have an array of stages, where each stage has a `stageThreshold` and its own array of `weakClassifiers`. The elements of each weak classifier merit further explanation:

- `featureRectangle`: Gives the position and dimensions of the weak classifier's Local Binary Pattern feature as a tuple $(x, y, width, height)$. The (x, y) coordinates give the top left corner of the feature, and the width and height are those of a single block of the feature, as shown in Figure 14.

- `leafValues`: The contribution of the weak classifier to the stage total in the case that it evaluates as negative (first value) or positive (second value). The stage total is the sum of these results for all its weak classifiers, and a stage passes if this total exceeds `stageThreshold`.

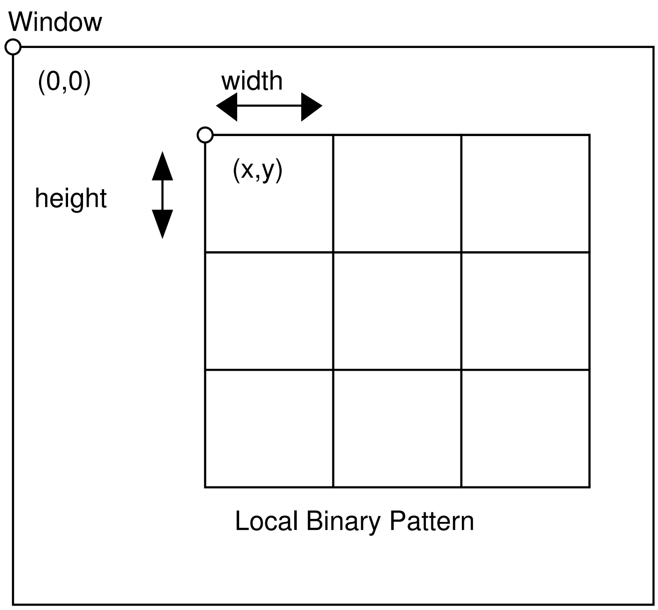

Figure 14: Interpretation of `featureRectangle` values

- `categoryBitVector`: Perhaps the most cryptic of the elements, this is a compact representation of which of the 256 possible Local Binary Patterns should be considered a positive result for the weak classifier, and which should be negative. It should be interpreted as eight 32-bit signed integers, giving 256 bits overall. This gives us a bit vector, where the i^{th} bit (counting from 0) is 1 if pattern i is negative and 0 if it is positive (using OpenCV's somewhat counterintuitive convention). For example, pattern 10101010_{bin} (which would represent alternating lighter and darker blocks than the centre) is 170 in decimal, and if this pattern were indicative of a face, then the 170^{th} bit in the bit vector would be 0. To check if bit i is zero or one, we can use the bitwise formula:
  `bitvec[i >> 5] & (1 << (i & 31))`
  which will be non-zero if bit i is set. This uses a right shift by 5 to select the three highest bits of i as an index to one of the 8 integers, then ANDs this integer with a number whose j^{th} bit (only) is 1, hence being non-zero if bit j of the integer is set. j is the lowest 5 bits of i and is obtained by masking i with 31 (11111_{bin}), and then to get a number whose j^{th} bit is 1 we left shift 1 by j.

This representation of the weak classifiers is in fact a simplification over that used in the original OpenCV XML file, which uses a rather vaguely named `<internalNodes>` element containing, in order, two dummy pointers to child nodes (unused, since we are dealing with a stump based classifier, containing only two leaf nodes, rather than a tree), the index of the feature rectangle (number 46 in example below) which is used to look up the actual rectangle specified elsewhere in the XML file, and then the eight elements of the bit vector.

```
<weakClassifiers>
  <!-- tree 0 -->
  <_>
    <internalNodes>
      0 -1 46 -67130709 -21569 -1426120013 -1275125205 -21585
      -16385 587145899 -24005</internalNodes>
    <leafValues>
      -0.6543210148811340 0.8888888955116272</leafValues></_>
  ...
```

Given this specification of the weak classifiers, we now look at how to compute the corresponding Local Binary Pattern values. From the `featureRectangle` associated with each weak classifier we can find the position of the blocks of our Local Binary Pattern within the window. In order to compute the Local Binary Pattern value we need to know the total intensity of each of these blocks (ie, the sum of all the grayscale 0-255 pixel values). By using the integral image, we can find the intensity of a block of any area with just four integral image values, those at the corners. We have nine blocks in a pattern, but some share corners, so we require 16 points in total, shown in Figure 15.

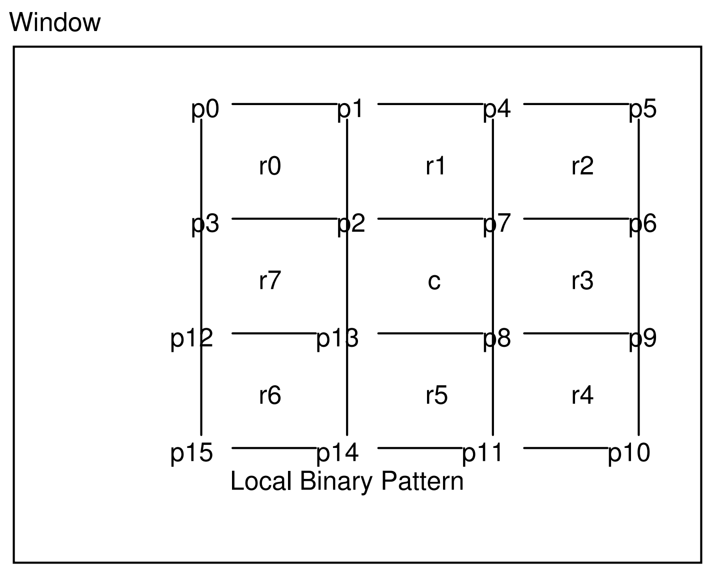

Figure 15: Points looked up for LBP (p0-15) and regions whose intensity we require (r0-7 and c)

Computing the total intensities is then just a matter of using the integral image trick described in [TODO], which takes advantage of the fact that the value of the integral image at each point is the sum of all pixels to the top- left of it in the original image. For example, for the centre and first block we have:

```
c = p8 - p6 - p13 + p3;
r0 = p3 - p2 - p1 + p0;
```

Then, to find the value of our Local Binary Pattern as an 8-bit number, we must ask whether the value of r0 through to r7 is greater than the centre value c. If we define bit b_i as the result of the expression $r_i \geq c$ (where true=1, false=0) then our binary value will be $b_0b_1b_2b_3b_4b_5b_6b_7$, which can be computed in JavaScript using bitwise shifts and sums.

With this JavaScript implementation of the cascade we can now observe graphically the effect of each stage, by drawing masks of which windows are accepted or rejected, plotting a white or black pixel respectively at the top- left position of each window. This lets us see the early termination effect which the cascade provides, whereby only a small number of windows pass through to the end, saving computational effort. We can also plot the 0-255 values of the Local Binary Patterns, giving a visualisation of their distribution over the image.

[TODO lbp and mask images, speed]

Adapting to WebGL

Having completed a reference implementation in JavaScript, it is now time to consider how best to take advantage of the capabilities of WebGL in order to speed things up. We have seen [TODO] how WebGL can be used for computation on a grid, and this method adapts itself quite naturally to our need to compute many windows, whose results are independent of each other.

The main strategy for the initial implementation of face detection in WebGL is to offload the computation of each stage, involving the lookup operations on the integral image, the calculation of the Local Binary Pattern values, and the subsequent window evaluation to the fragment shader. This allows the “sliding window” to be parallelised so that we are evaluating multiple window positions at once.

Since the classification of a window requires the evaluation of a number of stages, one choice we must make is whether to evaluate all these stages at once, looping over each stage within the fragment shader, which would require a single shader program able to handle every stage, or whether we should break up the evaluation into a different draw call per stage, keeping track of which windows have passed the previous stages using a texture.

Although having a single monolithic shader would avoid the overhead of a separate draw call for each stage, there are reasons not to prefer this approach.

Firstly, we are limited in the amount of Uniform variables we can transfer to the shader. According to WebGLStats (2013) 81% of users have a maximum of 221 Uniform 4-component variables available in the fragment shader, although for 9% of users it is as low as 29. (These limits, which can be queried at runtime, give the number of vectors of 4 floats which can be used. Quite how this corresponds to limits on other types and arrays does not seem to be documented, but they would be expected to share the same registers so be similarly limited, and there is some (desktop OpenGL) discussion in Krumlinde (2011)) At 20 stages, each having up to 10 rectangles, we would struggle with these limits. We could resort to packing the data into textures, however another limitation is that loop conditions and array sizes in GLSL must be based on constant expressions, available at compile time. Since each stage has a different number of weak classifiers, we would want to loop over a different number at each stage. We could solve this with a branch or `break;` within the loop, however branching carries with it performance penalties. [TODO branching appendix]

By instead having a shader program for each stage, we can use the same source code for each stage, but inject compiler `#define`s specifying certain constants, such as the stage number and the number of weak classifiers in the stage, allowing us to use constant expressions for loop conditions. We can then also make use of preprocessor directives so that different code is compiled for different stages. Since GLSL has no array literals, we still need to upload the arrays of `leafValues` and `featureRectangles` as Uniform arrays, but because their size will be determined by the number of weak classifiers in a single stage (maximum 10), we avoid pushing the limits of Uniforms allowed. One disadvantage of having many shaders is that we must compile them all, which gives a small delay upon initialising the face detector (around a second for the 20 stages), however this is a one-time cost upon startup so not too important for most applications.

Each stage writes out a texture with a white pixel for each window accepted, a black pixel otherwise. The texture from the previous stage is used as an input to the next stage, to avoid computing windows which have already been rejected. An additional advantage of splitting the computation into multiple draw calls is that we can inspect these intermediate textures in order to debug our code.

For each stage in the face detection cascade we have to compute the Local Binary Pattern value for various weak classifiers within the window. Depending on which pattern we get for a rectangle, it may either contribute a positive or a negative weighting towards the window being a face. Summing the weights contributed by all the rectangles and comparing against an overall threshold for the stage, we determine whether the window should be rejected outright or subjected to further scrutiny in later stages. Computing each Local Binary Pattern rectangle requires 16 texture lookups, since we have to subdivide the rectangle into 3x3, giving 9 blocks, and compare the intensity of the centre block with the 8 surrounding blocks. Using the integral image technique, finding the intensity of a block of any area requires just four texture lookups.

The data on which Local Binary Patterns should be considered positive or

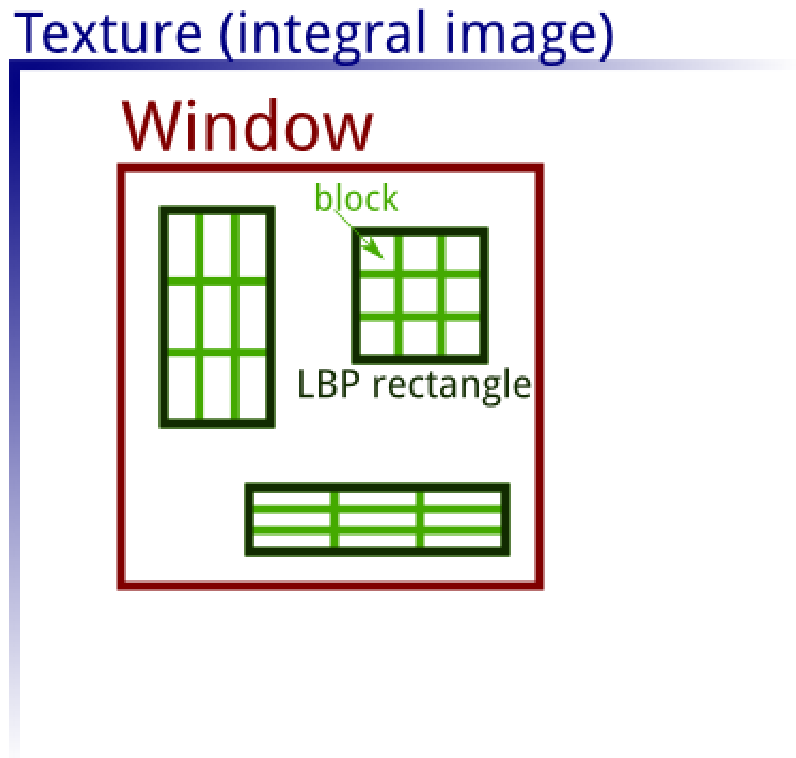

Figure 16: Window for a stage with 3 rectangles

negative is accessed from the shader by using a grayscale texture as a lookup table. There is one row for each stage in the cascade, so the height is the number of stages, and for each LBP rectangle we have 256 possible patterns. A black pixel is used to indicate a positive pattern, a white pixel a negative pattern. The width of the texture is then 256 x the maximum number of rectangles. For the default cascade used, we have 20 stages and a maximum of 10 LBP rectangles, giving a 10×2560 texture. This differs from the more compact representation used by OpenCV, which packs the data for one rectangle into 256 bits (8 32-bit ints) per rectangle but is necessary because the GL shader language does not support the bitwise operations needed to extract the individual bits (since numbers may in fact be implemented as floating point in hardware), nor the range needed for 32-bit integers.

Scaling

On top of this loop over stages, we also need to consider different scales, to be able to detect faces of different sizes in the image. This is done by setting a scale factor, such as 1.2, which we successively multiply the window size and rectangle offsets by. We run the detection for each scale, starting from the base 24x24 pixel window size, until some maximum where the window would be too big to fit in the image.

After detection is run on each scale, the accepted window texture is read back to a JavaScript array using the WebGL `gl.readPixels` command, and used to draw appropriately sized rectangles at the locations where faces have been found.

TODO: scaling vs opencv

Optimising

Achieving Higher Performance

In order to test how fast this initial implementation is we can insert some timer calls. We measure the time for each scale as well as the overall time for the detection call (after the inital setup of shaders and textures), on an image of dimensions 320x240 containing three faces of different scales. This gives the output shown below.

This gives an overall time of 375 milliseconds, obviously not good enough for real time detection. Looking more closely, the majority of time seems to be spent on the first scale, which takes 212 ms, whereas the other scales take 10ms or less. Using the Chrome Javascript Profiler tool we can investigate further by checking which functions are taking up the most time.

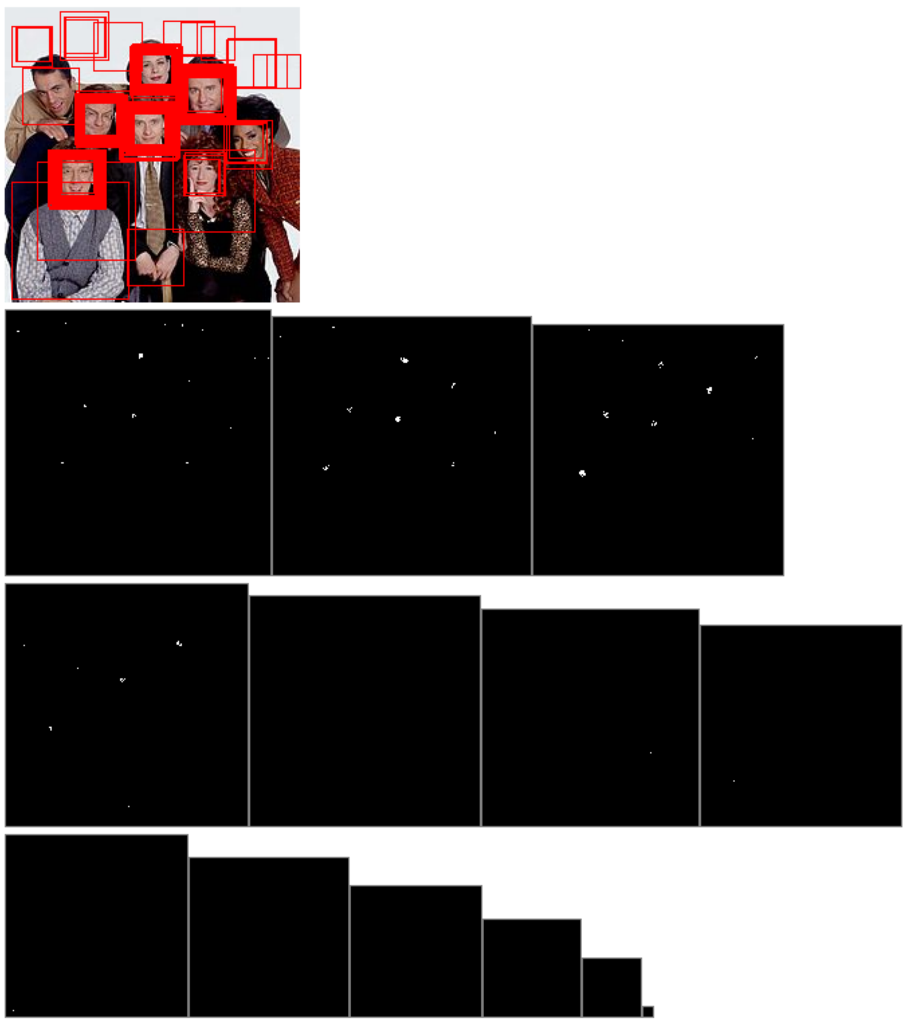

Figure 17: Output of detection at different scales

```
Scale 1 time 212
Scale 1.2 time 9
Scale 1.44 time 8
Scale 1.728 time 10
Scale 2.0736 time 8
Scale 2.48832 time 9
Scale 2.9859839999999997 time 8
Scale 3.5831807999999996 time 9
Scale 4.299816959999999 time 7
Scale 5.159780351999999 time 5
Scale 6.191736422399999 time 5
Scale 7.430083706879999 time 4
Scale 8.916100448255998 time 3
number of draw calls: 260
Overall time: 375
```

Figure 18: Initial timing

Self	Total	Function
3.00 s	3.00 s	(idle)
469 ms	509 ms	▶ compileShaderProgram
242 ms	242 ms	▶ readPixels
230 ms	230 ms	(program)
59 ms	336 ms	▶ FaceDetector.detect
27 ms	27 ms	(garbage collector)
26 ms	26 ms	▶ IsSendRequestDisabled
24 ms	34 ms	▶ jQuery.extend.style
20 ms	20 ms	▶ getProgramParameter
17 ms	17 ms	▶ getContext
16 ms	16 ms	▶ getShaderParameter
11 ms	22 ms	▶ showRGBA
8 ms	12 ms	▶ jQuery.fn.jQuery.init
8 ms	8 ms	▶ jQuery.extend.camelCase
7 ms	7 ms	▶ set src
6 ms	13 ms	▶ jQuery.buildFragment
6 ms	17 ms	▶ jQuery
6 ms	6 ms	log

Figure 19: Javascript Profile

This shows that (besides the initial overhead of setting up the shaders) most of the time is spent in the `gl.readPixels` function, responsible for transferring image data from GPU memory back to JavaScript. An easy way to see just how responsible this function is for the slowdown is to simply comment the `readPixels` calls and associated code for drawing rectangles, which gives the following timings:

```
Scale 1 time 0
Scale 1.2 time 1
Scale 1.44 time 0
Scale 1.728 time 0
Scale 2.0736 time 0
Scale 2.48832 time 0
Scale 2.9859839999999997 time 0
Scale 3.5831807999999996 time 0
Scale 4.299816959999999 time 0
Scale 5.159780351999999 time 1
Scale 6.191736422399999 time 0
Scale 7.430083706879999 time 0
Scale 8.916100448255998 time 1
number of draw calls: 260
Overall time: 8
```

Figure 20: Timing without readPixels

This shows a massive improvement, bringing the time down to 8ms, but obviously our face detection is not very useful if we cannot actually get the locations of the faces at the end!

The previous results were timed using a single image, running the detection once after the page loads. In a real scenario we would want to be detecting continually on each frame. This leads us to investigate the result of running the detection on two different images, one after the other, without refreshing the page. (In fact the same image, but flipped horizontally, so we would expect similar face detection results, but avoid any clever caching by the browser).

This gives the surprising result that, while the first run of the detection takes a long time, the second is considerably shorter, with times between 2 and 10 ms for each scale. While we cannot determine the exact cause of this, it seems that from a "cold start", readPixels has some overhead which is not experienced on subsequent calls. So while readPixels is still the slowest factor, once the detection gets going we need not worry about reads taking over 100ms. From here, the best strategy to improve overall time seems to be to minimise the number of readPixels calls needed, ideally with just one at the end of detection rather than intermediate calls for each scale.

While refactoring the code to "pingpong" by flipping between multiple framebuffers, rather than the more expensive technique of using one framebuffer and

Image 1	Image 2
Scale 1 time 221	Scale 1 time 9
Scale 1.2 time 8	Scale 1.2 time 8
Scale 1.44 time 9	Scale 1.44 time 10
Scale 1.728 time 9	Scale 1.728 time 8
Scale 2.0736 time 9	Scale 2.0736 time 8
Scale 2.48832 time 9	Scale 2.48832 time 8
Scale 2.9859839999999997 time 12	Scale 2.9859839999999997 time 7
Scale 3.5831807999999996 time 6	Scale 3.5831807999999996 time 7
Scale 4.299816959999999 time 5	Scale 4.299816959999999 time 7
Scale 5.159780351999999 time 4	Scale 5.159780351999999 time 6
Scale 6.191736422399999 time 3	Scale 6.191736422399999 time 6
Scale 7.430083706879999 time 3	Scale 7.430083706879999 time 5
Scale 8.916100448255998 time 3	Scale 8.916100448255998 time 2
number of draw calls: 260	number of draw calls: 260
Overall time: 367	Overall time: 151

Figure 21: Timing on two images

attaching different textures in turn (as recommended by Tavares (2011a) at 37m20s), it was discovered that the slowdown on the first readPixels seemed to disappear. However, after some work to narrow down the exact conditions which would produce the slowdown, it was determined that this optimisation alone was not responsible for the difference, but rather that it was determined by the ordering of the calls to attach textures to the framebuffers, relative to the code setting up the shaders. It turned out that, if at least one `gl.framebufferTexture2D` call was before the shader setup, the initial readPixels call took 10ms, whereas otherwise it took over 200ms. The initial setup which includes compiling the shaders always takes around half a second, so while the order of calls does not change the initial setup time, it allows the "warm up" time required before readPixels to effectively be hidden behind the time needed to compile the shaders. This is likely because the shader compilation is mostly CPU-bound, allowing other tasks to be done in parallel on the GPU.

In order to eliminate the intermediate readPixel calls, we need to write the output from each scale to the same texture, preserving the pixels output from the previous scale, and encoding the scale in the pixel value. To indicate the scale of an accepted window we can simply write out the ordinal number (1,2,3…) of the scale as a colour value, or 0 if the window is rejected. The size to multiply the rectangle by is then $scaleFactor^{(scaleNumber-1)}$. The use of two textures to "pingpong" the results between each stage in a scale remains as before, except that on the final stage we write to a shared final output texture. One limitation is that, if we have two detections of different scales at exactly the same position, the later (larger) scale will overwrite the previous one. However, this should be a relatively rare occurence, and should not make too much difference when all the rectangles are grouped to find the final face positions. Another complication is that we want to keep the previous written pixels, instead of writing a black pixel for a rejected window in a subsequent scale. The simplest way to prevent output of any pixel at all is to use the `discard;` statement in the fragment shader. However, in certain cases (discussed in Jave (2011)) this may invoke a performance penalty, particularly on mobile GPUs. An alternative is to use OpenGL's blend modes, which specify how pixels written should be blended with the pixels already present.

Figure 22: Writing out pixels for each scale. A lighter colour pixel indicates a larger detection

First an implementation was created using `discard;`, giving an average time of 71ms per detection run (for a 320x240 image over 20 runs), compared to 110ms using `readPixels` for each scale under equivalent conditions.

The implementation was then adapted to use blending, in order to test which would give the best performance. As explained in Thomas (2009), the `gl.blendFunc(sfactor, dfactor)` function sets the factors which the source (being drawn) and destination (already in the framebuffer) should be multiplied by, where `sfactor` and `dfactor` are symbolic constants determining where the factors should come from. The output for each colour channel is given by $Result = SourceVal \times SourceFactor + DestVal \times DestFactor$. We set `sfactor` to `SRC_ALPHA` and `dfactor` to `ONE_MINUS_SRC_ALPHA`, which means that when outputting `gl_FragColor` we can set the alpha value to 0.0 to completely preserve the existing pixel.

Comparing the timing of the two techniques over 100 iterations, there turned out to be almost no difference in the mean time, at least on a laptop Intel GPU, although as shown in the box plot the Blend version had a slightly greater variance. In the end the Blend version was preferred, to avoid potential slowness with other GPUs and because it allowed the shader code to be simplified, eliminating a branching condition to explicitly check if the window was rejected.

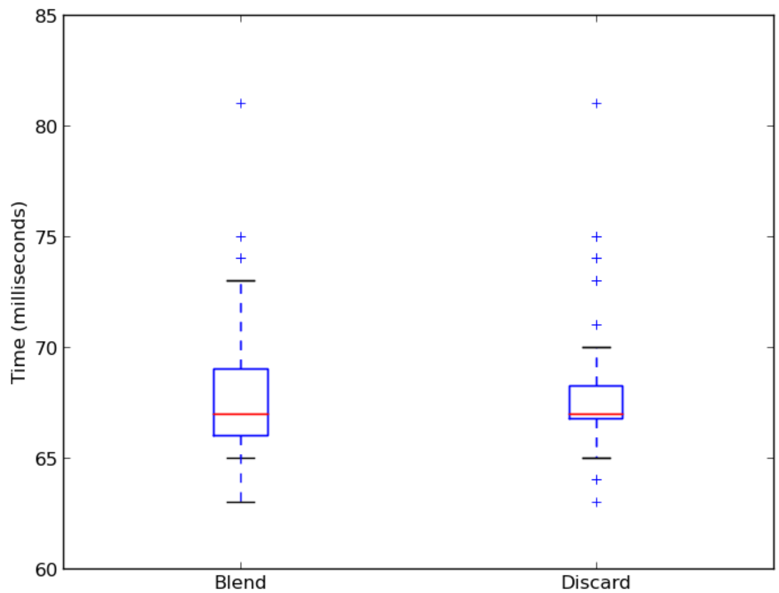

Figure 23: Box plot of timings using Discard vs Blend, for 100 iterations

Timing stages

In order to analyse the times of operations at a finer granularity, we want to time each draw call individually. However, because the CPU and GPU operate asynchronously, each draw call will in fact return immediately, and the CPU will only wait for the GPU to finish when some operation requiring information from a framebuffer is performed. Therefore, we insert a dummy readPixels operation, reading only 1 pixel, after each draw. Because some times are very small (below 1ms) and difficult to measure accurately, we also artificially repeat each draw operation 10 times, and divide the total time by 10. In this way, we can obtain a detailed profile of how much time is spent running the shader for each stage and scale.

We observe that, as expected more time is spent in the early stages, because the first stage must run on all windows, whereas for laters stages some windows are rejected. Increasing the scale also shows a decrease in time, since less window positions need to be evaluated, although this is only really noticeable in the first two stages, the subsequent stages showing around the same time regardless of scale.

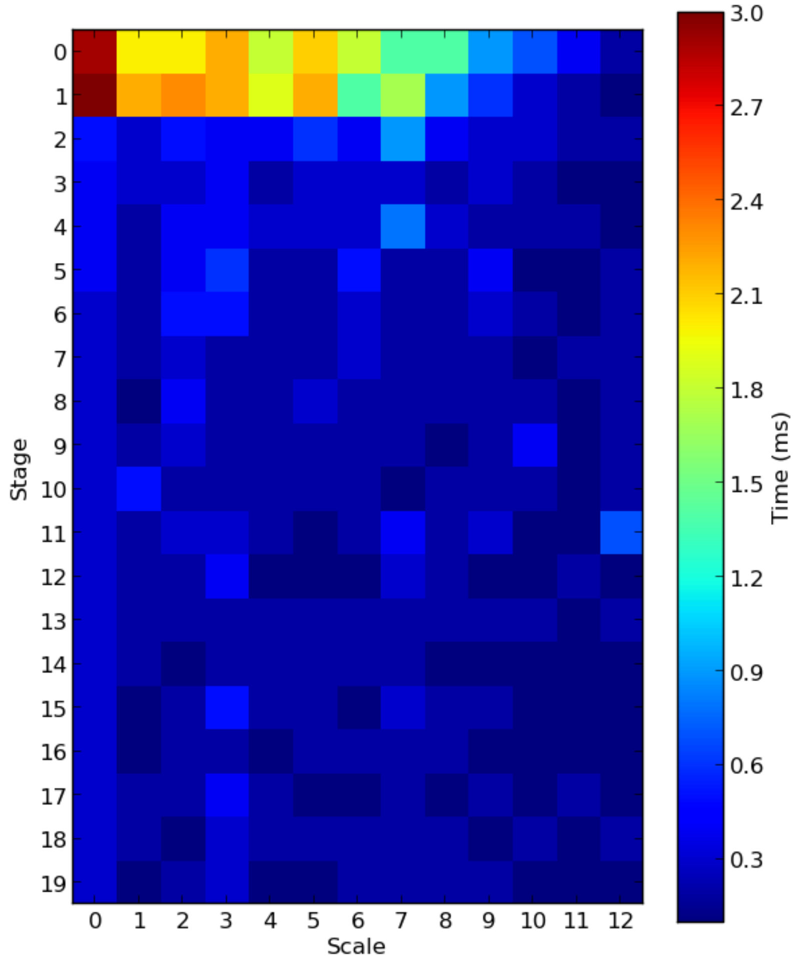

Figure 24: Times of stages and scales

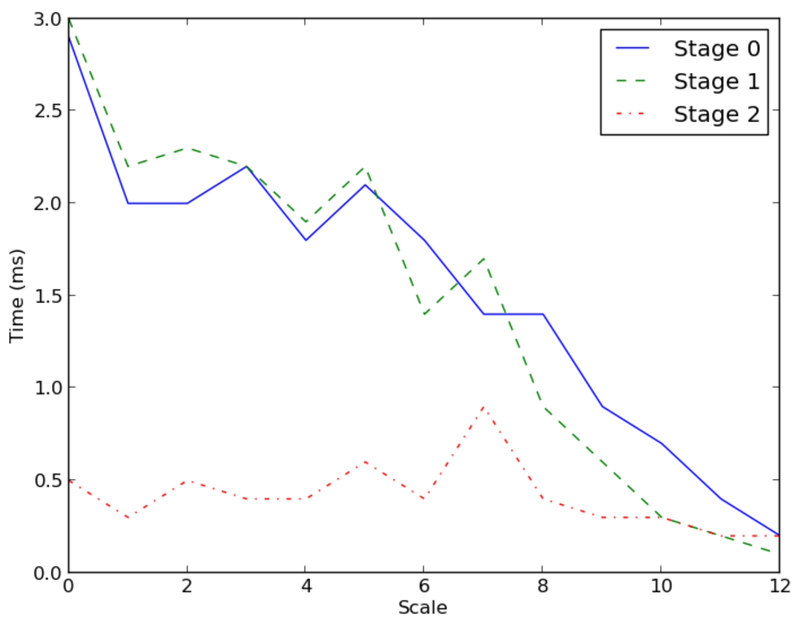

Figure 25: Times for the first 3 stages at different scales

What is interesting to note is that the first three stages take up 48% of the time, while the remaining 17 stages take up 52% of the time. So while it is tempting to try to chip away at the above-2ms times in the early stages, we have a "long tail" effect where the sub-0.5ms times of later stages add up to a significant proportion of the overall time. Therefore, treating the early stages as special cases (such as manually fine-tuning the shader code for these specific stages) is unlikely to provide much of an advantage, compared to general techniques that apply equally to the later stages.

Why are the shaders slow?

At an abstract level, all the fragment shaders are doing is

1. Looking up some values in the integral image and LBP lookup textures
2. Doing some maths to determine what value to output

Now, GPUs are typically very fast at carrying out floating point calculations, so we wouldn't expect the "maths" portion to be overly challenging. Harris (2005) explains this using the concept of "arithmetic intensity", the ratio of computation to bandwidth.

```
arithmeticIntensity = operations/wordsTransferred
```

According to Harris, applications that benefit most from GPU acceleration are those with high arithmetic intensity, where "The data communication required to compute each element of the output is small and coherent". So ideally, the amount of data fetched from textures would be small, and would be spatially localised, in order to take advantage of caching. Unfortunately, in order to calculate the 9 blocks of the rectangle for each classifier, we require 16 texture lookups, and the positions fetched for a window are not guaranteed to be close together. Since the number of weak classifier rectangles can vary from 3 in the first stage to 10 in the later stages, we are talking about $3 \times 16 = 48$ at best and $10 \times 16 = 160$ at worst texture lookups. For the base scale they will at least be within the same 24×24 area, but when the window is scaled we will be fetching values locations more spread out over the image. Texture caches are typically optimised for some 2D neighbourhood of a few texels, which great for applications such as convolution where we just need to look up adjacent texels, but is not ideal for more general purpose approaches.

To test the theory that the texture fetches are responsible for most of the slowdown, we create a test shader which performs the same texture fetches as our face detection shader but does not do anything useful with the result (instead just outputting the sum of the values, to ensure the fetches are not optimised out). Performing the same texture fetches as the 1st stage of the cascade (48 fetches), and timing over 1000 iterations, we get an average time of 3.1 ms per draw call, which is pretty much identical to the full shader. Further, commenting out half the fetches reduces the time to 1.3ms, clearly showing the impact of texture fetching on the time.

TODO: Things tried that made no difference:

- Moving code to calculate rectangle offsets into vertex shader
- Using UNSIGNED_BYTE texture (is faster if just reading one component (byte), but once we access all it is just as slow as FLOAT texture)
- Iterating over scales within the shader (just made the “multiscale” shader around as slow as the combined time for different scales, and makes it difficult to track which windows accepted, since we need to encode for each scale somehow)

Z-Culling

z-Culling: use the depth buffer to indicate rejected windows, so that the fragment shader doesn’t run at all for these pixels. This offers some speedup by not running fragment shader at all on blocks of some size, and will avoid having to read the “activeWindows” texture.

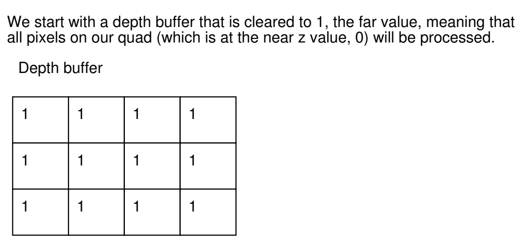

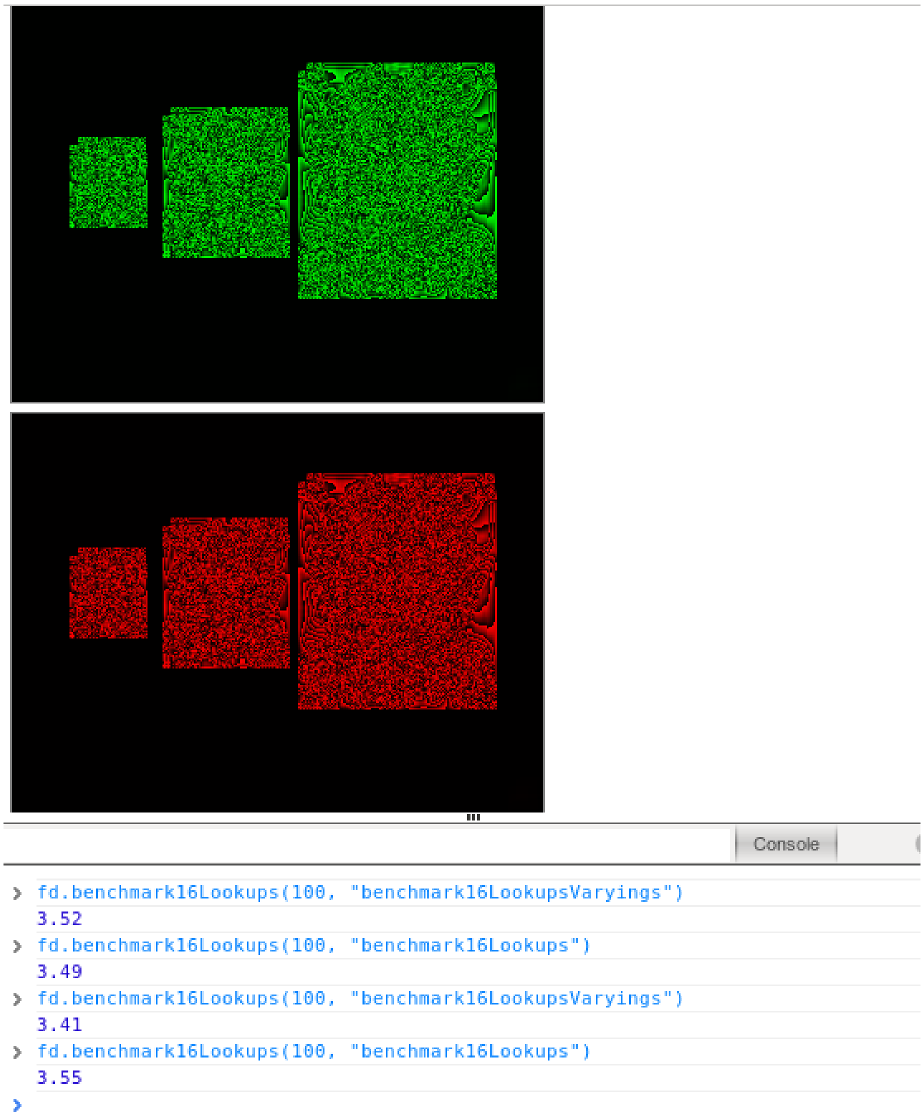

Figure 26: Calculating offsets for texture lookup with varyings in the vertex shader (green) vs fragment shader (red) gives no difference in timing, around 3.5ms in each case. The output values are simply the sum of all texture values mod 255, giving not very meaningful output, but showing that identical values are computed

We then run the first stage, which will discard the output if the window is accepted, writing a 0 if it is rejected. This causes the depth buffer to be updated to the z value of the quad, 0, for those windows which have been rejected, whereas the previous depth of 1 is preserved for the accepted windows, since their output is discarded.

1st Stage Output
d discarded
1 rejected

d	0	d	0
0	d	d	0
0	0	d	0

Updated depth buffer

1	0	1	0
0	1	1	0
1	1	0	1

On subsequent stages, those pixels with a depth value of 0 will not be processed, since we are using the "gl.LESS" depth test to compare the depth of the pixel on our quad with the depth in the depth buffer, and because zero is not less than zero, the test fails, so the pixel is not processed.

2nd Stage Output
x not processed
d discarded
1 rejected

d	x	0	x
x	0	d	x
x	x	0	x

Updated depth buffer

1	0	0	0
0	0	1	0
1	1	0	1

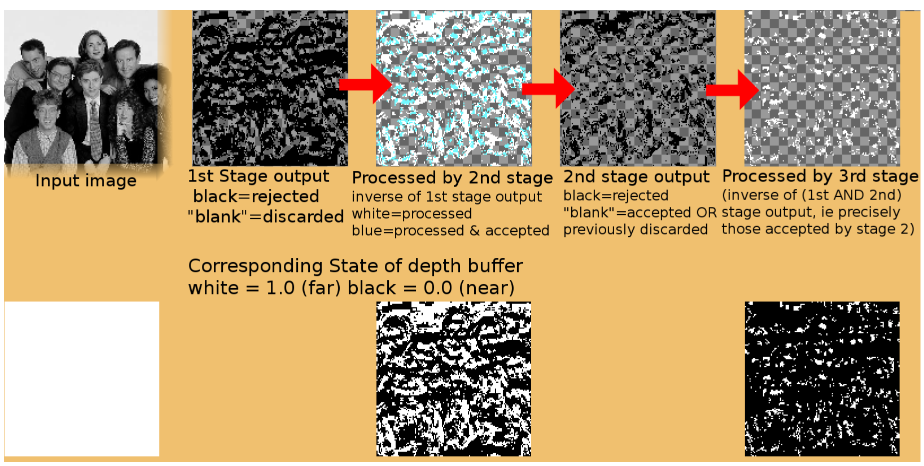

Figure 27: An illustration of Z-culling on an actual image. We use a checkerboard pattern to show the lack of a value

Evaluation

Application for Head Tracking

Grouping Rectangles

Tracking

Kalman Filter

Our head tracking gives a fast, responsive result allowing the user to quickly observe the 3D scene from different angles. However it suffers from the problem of jitter in the camera position, due to small shifts in the precise pixel location of the detected face, even when the head remains fairly stationary. These noisy measurements are an unavoidable aspect of our detection, but we can employ some filtering to get a smoother result.

The Kalman filter is a Bayesian hidden variable [TODO is it?] model which can be used to estimate the dynamics of a system, with a linear Gaussian transition. The typical example is that of tracking blips on a radar, estimating position and velocity from these noisy observations. The Kalman filter consists of determining the mean and covariance of a gaussian distribution through a cycle of measurements, updates, and predictions.

We shall start with a simple 1D example.

Assume we have a prior $P(x_t) = N(x_t; \mu_t, \sigma_t^2)$. The mean and variance for the prediction at the next time step, $P(x_{t+1})$ are given by the rules:

$\mu_{pred} = \mu_t + \mu_{motion}$

$\sigma_{pred}^2 = \sigma_t^2 + \sigma_{motion}^2$

Where μ_{motion} lets us specify some external motion in the system (but we can simply set it to zero) and σ_{motion}^2 (the motion noise, or transition variance) is some constant variance specifying our uncertainty in the motion, ie how unpredictable we expect it to be.

We then make a measurement, z and consider the posterior distribution

$P(x_{t+1}|z)$

The posterior mean and variance are given by the Kalman update step:

$\mu_{t+1} = \frac{\sigma_{pred}^2 z + \sigma_{measure}^2 \mu_{pred}}{\sigma_{pred}^2 + \sigma_{measure}^2}$

$\sigma_{t+1}^2 = \frac{\sigma_{measure}^2 \sigma_{pred}^2}{\sigma_{measure}^2 + \sigma_{pred}^2}$

Where $\sigma_{measure}^2$ is our measurement noise, a constant variance giving our uncertainty in the measurement.

Russel & Norvig (2010, chap.15 p. 587) explain how σ^2_{motion} and $\sigma^2_{measure}$ control the tradeoff between our predicted and measured values. The update μ_{t+1} can be seen as just a weighted average of the prediction μ_{pred} and the measurement z, with the two variances giving the weights. If we are not very confident in the measurement, then $\sigma^2_{measure}$ will be large and we will prefer the predicted value. However if we doubt the old mean (high σ^2_t) or our motion is unpredictable (high σ^2_{motion}) then σ^2_{pred} will be large so we prefer the measurement z. This effect can be seen graphically in Figures 28 and 29.

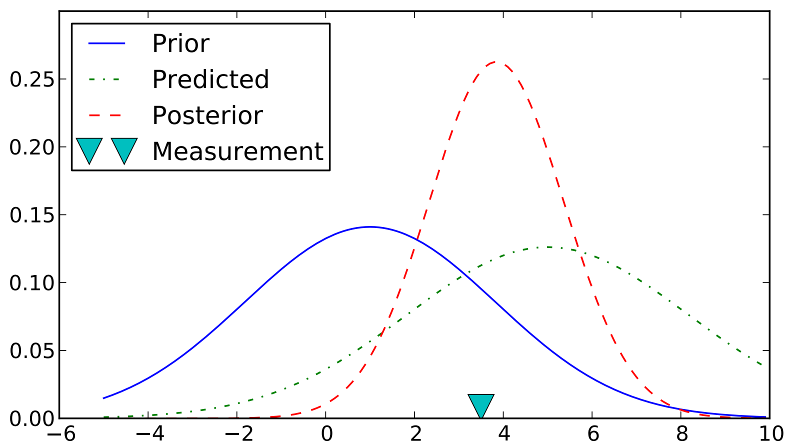

Figure 28: The update cycle for 1D Kalman with prior mean 1 and variance 8, and external motion shifting the prediction mean right by 4. Motion noise $\sigma^2_{motion} = 2$, measurement noise $\sigma^2_{measure} = 3$ and the measured value is 3.5. Notice how the width of the posterior decreases, indicating an increase in certainty. The mean of the posterior is 3.85, slightly to the right of the measured value, due to the weighted average effect between the prior and prediction.

The general, multivariate case of the Kalman filter is more complicated, involving some intimidating linear algebra, which we will not explain in detail, but only give a brief overview. For 2D motion, our mean now becomes a state containing the positions and velocities in each direction, $x = (X, Y, dX, dY)^T$, and our variance is now a covariance matrix P. The motion noise and measurement noise are now matrices Q and R, for which we can specify values along the diagonal giving the noise for each variable.

- The prediction step:
  New State $x' = Fx + u_{extmotion}$
  New Covariance $P' = FPF^T + Q$
- Update with measurement z:

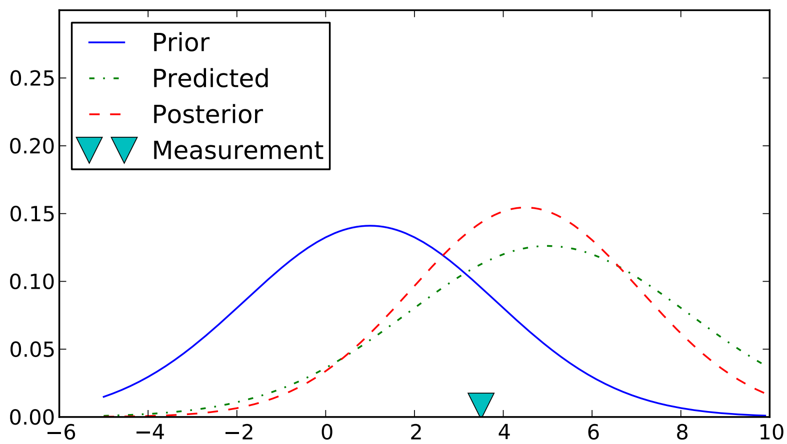

Figure 29: Changing the measure noise, $\sigma^2_{measure}$ from 3 to 20 has the effect of pulling the posterior towards the predicted value and away from the unreliable measurement.

Innovation $y = z - Hx$

Residual covariance $S = HPH^T + R$

Kalman Gain $K = PH^TS^{-1}$

New State $x' = x + Ky$

New Covariance $P' = (I - KH)P$

The matrix F is our state transition function, giving a linear transformation of our state x. For calculating the 2D dynamics we want to set F to

```
F = 1 0 1 0
    0 1 0 1
    0 0 1 0
    0 0 1 0
```

Which means `x<-Fx` causes the update:

```
X  <- X + dX
Y  <- Y + dY
dX <- dX
dY <- dY
```

The matrix H is the measurement function, which "picks out" the measured values from the state.

```
H = 1 0 0 0
    0 1 0 0
```

Where $H \times (X, Y, dX, dY)^T = (X, Y)^T$, selecting the two positions.

In order to apply the Kalman filter for reducing the noise in measured face positions, we implement a Kalman filter in JavaScript, using the Sylvester matrix library. To demonstrate this we apply the filter to mouse clicks on a webpage, shown in Figure 30.

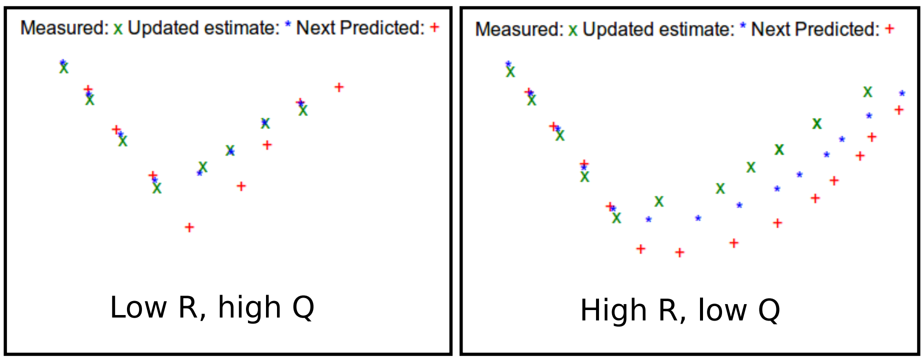

Figure 30: Kalman filter in Javascript, tracking mouse clicks. The lower R (measurement noise) and higher Q (motion noise) causes there to be more certainty in the measured clicks, so the updated states remain near the clicked position. For the opposite case, the estimates are "pulled" towards the prediction.

We use a Kalman filter to track the 3D dynamics of the face, where the Z coordinate is given by the width of the window. The result is that the camera movements in the 3D scene are a lot less subject to noise. We can tweak the parameters R and Q to determine the extent of this effect. Setting a low Q means that the motion is smoother, but the virtual camera reacts less quickly to sudden movements, and with a very low value it can feel like your head is "pulling" the camera around with a piece of elastic. A high Q means it is more responsive, but there is a perceptible "jiggle" in the camera position caused by the noise.

When we fail to detect the face in the image, we can skip the Kalman update from a measurement and just use the predicted position. This allows the camera to continue moving at the same constant speed. We do this for 10 frames before giving up, in case the face reappears, so that the camera motion is not interrupted if we lose the face for a couple of frames.

Further Work

Optimisations to look at:

- "Stage-parallel" processing - compute weak classifiers over a larger window at once, as in Obukhov (2011) - problem: Can only output four bytes for each fragment
- Split some work between CPU and GPU. Since the different scales can be computed independently, could hand off some portion of the scales to CPU to be processed simultaneously (but would then lose ability to use CPU for other tasks)
- Reduce number of texture accesses by "factorisation" of the LBP pattern - eg if we know the top left block should never be zero, can return negative from classifier after just computing centre and top left blocks. Problems: branching, and how to represent the "factoring" data in the shader (if it requires fetching more values from texture could do more harm than good!)

Appendix

Coordinate Considerations

Working with the OpenGL ecosystem invariably requires an understanding of the different coordinate systems used for the polygon vertices, textures and screen. This becomes even more important when using OpenGL for computation, as being off by one pixel (or a fraction of a pixel) can have much more serious consequences than mere graphical glitches. If a texture is used as a lookup table for arbitrary information, it is essential that the correct values are indexed, to avoid giving, at best, completely incorrect results, or at worst hard-to-detect bugs due to the limitations of floating point precision in the 0 to 1 range used to index textures.

Firstly we have the window (or screen) coordinates, which give the position in the viewport, in other words the final image output. However, since the output may be rendered to a texture, window coordinates don't have to be related to an image actually displayed on the screen. They are similar to pixel positions, however OpenGL itself does not have a concept of a pixel until rasterisation. Peers (2002) gives a detailed mathematical treatment of OpenGL coordinates, drawing from the OpenGL specification. In this way, the viewport can be treated as a Cartesian plane whose origin and unit vectors are given by the `gl.viewport(x,y,w,h)` command. This sets the x,y offset of the origin, which is at the bottom-left edge of the image, and determines the area of the scene which should be rasterised, so in a graphics sense can be considered a sort of cropping of the image. Two important points to note here are that the Y axis is effectively flipped relative to the coordinate system usually used in graphics, which has the origin at the top-left, and that integer coordinates will index the bottom left corners of pixels, so to index the centre of a pixel requires adding 0.5 to each dimension. For general purpose computation on a grid, modifying the viewport can be used to change the output range of the computation. For example, when doing face detection at different scales, the "sliding window" of the detector will change size, meaning less pixel positions need to be considered for larger windows, so the size of the output grid should be smaller.

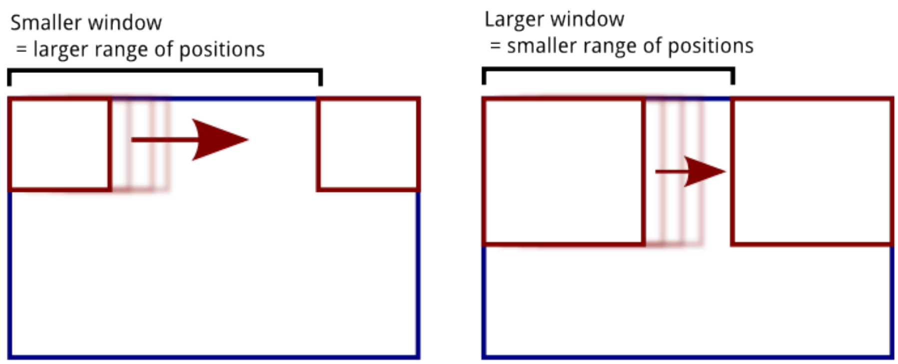

Figure 31: Decreased output range for larger window

The vertex positions of polygons are specified by setting the `gl_Position` variable in the vertex shader. This is a four dimensional `(x,y,z,w)` vector where x,y,z are in Normalised Device Coordinates, a resolution-independent coordinate system which varies from -1 to 1 in each dimension such that the origin is at the centre. These then undergo perspective division by the fourth `gl_Position.w` coordinate. For convenience we can use window coordinates when we supply the vertices as an attribute, then compute the normalised coordinates in the vertex shader by dividing by the image resolution. This will give a value in the range [0,1], which can be changed to the range [-1,1] by multiplying by 2 then subtracting 1. For the purposes of computation on a 2D grid, the only geometry we need is a rectangle aligned with the viewport, which we can get by drawing two triangles. We do not want any perspective division, so z,w can be set to 0,1. This effectively "passes through" the vertex coordinates, allowing us to use them as if they were window coordinates.

The shader code to achieve this is: (where aPosition is the vertex position attribute and uResolution gives the image resolution)

```
vec2 normCoords = ((aPosition/uResolution) * 2.0) - 1.0;
gl_Position = vec4(normCoords, 0, 1);
```

Finally, we have to deal with the coordinates of texture maps, made up of texels (the texture equivalent of a pixel) which are sampled using texture2D() in the fragment shader. They have coordinates from 0,0 in the bottom left to 1,1 in the top right. Textures may be sampled using different filtering methods in order to interpolate between the discrete texels, the simplest being “NEAREST” which simply uses the closest texel value, and “LINEAR” which interpolates linearly based on the distance to surrounding texels. To sample at precisely the texel centre, with no filtering, it is necessary to offset by half a texel, since the “zero” of a texel is at the bottom left corner. So for the ith texel in a row we would use X coordinate `(i + 0.5)/width` to offset then normalise to the [0,1) range.

The Perils of Branching

Branching within the shader, while possible through the use of if-else statements, carries with it numerous caveats, explained in Harris & Buck (2005). In the “olden days” (say, 2003) in order to emulate branching, GPUs would simply evaluate both sides of the condition, then determine which result to use before writing the output. This meant that the time would be proportional to the cumulative cost of both branches.

Things got better with the SIMD (Single Instruction, Multiple Data) model, which uses multiprocessors executing the same instruction on many data elements at once. In this case, the GPU will not be doing useless work evaluating both sides of the condition, but instead divergent branches will cause a stall, where the processors that do not take a branch have to wait for the branching processors to catch up. In the worst case this will still take as long as both branches combined, but in the case where all processors take the same branch (known as coherency) it will be more efficient, and since the allocation of fragments to processors is often done in a spacially localised manner, it allows for speedups when fragments in the same area of an image branch in the same way.

Finally, true dynamic branching may be available in the form of MIMD (Multiple Instructions, Multiple Data) where different processors may execute different instructions simultaneously. Most modern GPUs support dynamic branching to some extent (NVIDIA’s GeForce 6 series, released in 2005, introduced MIMD branching in the fragment shader) however at an architectural level branching still presents a barrier to efficient parallel computation, since knowing that all fragments will follow the same instructions gives the GPU opportunities for optimisation.

For this reason, branching in the shader should be kept to a minimum, and it is preferred for algorithms to be structured such that fragments in the same neighbourhood take the same branches in order to maximise coherency. Especially in the case of WebGL, the programmer has no control over what graphics card capability the user will have, and is unable to query information about the graphics card due to security restrictions, so it is best to program for the lowest common denominator.

References

Bonext (n.d.) *flashopencv*. [Online]. Available from: https://github.com/bonext/flash-opencv.

Buck, I. (2005) Taking the Plunge into GPU Computing. In: Matt Pharr (ed.). *GPU Gems 2*. Addison Wesley. p. 509.

Harris, M. (2005) Mapping Computational Concepts to GPUs. In: Matt Pharr (ed.). *GPU Gems 2*. Addison Wesley. p. 493.

Harris, M. & Buck, I. (2005) GPU Flow-Control Idioms. In: Matt Pharr (ed.). *GPU Gems 2*. Addison Wesley. p. 547.

Harthur (n.d.) *Kittydar*. [Online]. Available from: http://harthur.github.com/kittydar/.

Inspirit (n.d.) *jsfeat*. [Online]. Available from: http://inspirit.github.com/jsfeat/.

Jave (2011) *Is discard bad for program performance in OpenGL? - Stack Overflow*. [Online]. Available from: http://stackoverflow.com/questions/8509051/is-discard-bad-for-program-performance-in-opengl [Accessed: 27th May 2013].

Khronos (n.d.) *WebGL_color_buffer_float Extension Draft Specification*. [Online]. Available from: http://www.khronos.org/registry/webgl/extensions/WEBGL_color_buffer_float/.

Khronos (n.d.) *WebGL_color_buffer_half_float Extension Draft Specification*. [Online]. Available from: http://www.khronos.org/registry/webgl/extensions/EXT_color_buffer_half_floa

Krumlinde, V. (2011) *GLSL: passing a list of values to fragment shader*. [Online]. Available from: http://stackoverflow.com/questions/7954927/glsl-passing-a-list-of-values-to-fragment-shader [Accessed: 16th June 2013].

Lab.dev.concord.org (n.d.) *WebGL GPGPU experiment - reading a floating point texture*. [Online]. Available from: http://lab.dev.concord.org/experiments/webgl-gpgpu/webgl.html.

Larson, B. (n.d.) *GPUImage*. [Online]. Available from: https://github.com/BradLarson/GPUImage.

Lienhart, R. & Maydt, J. (2002) An extended set of Haar-like features for rapid object detection. *ICIP02*. 900–903.

Liuliu (n.d.) *A Not-so-slow JavaScript Face Detector*. [Online]. Available from: http://liuliu.me/ccv/js/nss/.

Obukhov, A. (2011) Haar Classifiers for Object Detection with CUDA. In: Wen-Mei Hwu (ed.). *GPU Computing Gems*. Morgan Kaufmann. p. 517.

Ojala, T., Pietikhenl, M., Harwood, D. & Measures, L.T. (1994) Performance evaluation of texture measures with classification based on Kullback discrimination of distributions. *ICPR*. 582–585.

Peers, B. (2002) *OpenGL pixel and texel placement*. [Online] Available from: http://bpeers.com/articles/glpixel/.

Russel, S. & Norvig, P. (2010) *Artificial Intelligence A Modern Approach*. New Jersey, Pearson.

Tavares, G. (2011a) *Google I/O 2011: WebGL Techniques and Performance*. [Online]. Available from: http://www.youtube.com/watch?v=rfQ8rKGTVlg [Accessed: 27 May 2013].

Tavares, G. (2011b) *WebGL Fundamentals (WebGL is a 2D API!)*. [Online]. Available from: http://games.greggman.com/game/webgl-fundamentals/ [Accessed: 19th May 2013].

Tavares, G. (2011c) *WebGL Image Processing*. [Online]. Available from: http://games.greggman.com/game/webgl-image-processing/ [Accessed: 19th May 2013].

Thewlis, J. (2012) *Face Detection in Video for Digital Product Placement*. Industrial Placement at MirriAd Ltd.

Thomas, G. (2009) *WebGL Lesson 8 – the depth buffer, transparency and blending*. [Online]. Available from: http://learningwebgl.com/blog/?p=859 [Accessed: 27AD–May 13AD].

Viola, P. & Jones, M. (2001) Rapid object detection using a boosted cascade of simple features. *CVPR*.

Wallace, E. (n.d.) *WebGL Water*. [Online] Available from: http://madebyevan.com/webgl-water/.

WebGLStats (2013) *WebGL Stats*. [Online]. Available from: http://webglstats.com/ [Accessed: 16th June 2013].

Woolley, C. (2005) GPU Program Optimization. In: Matt Pharr (ed.). *GPU Gems 2*. Addison Wesley. p. 557.

Zhang, L., Chu, R., Xiang, S., Liao, S., et al. (2007) *Face Detection Based on Multi-Block LBP Representation*. 11–18.